

Modelling of spreading, imbibition and evaporation of liquids on structured or porous deformable substrates

1 State of the art and preliminary work

1.1 State of the art

Spreading of liquids over structured and porous substrates, liquid imbibition into porous layers as well as concomitant transport processes and phase change are important for many natural phenomena and industrial applications, including ink-jet printing, 3D-printing, penetration of rain drops into building walls, needleless injection, coating of porous materials, irrigation and cooling of electronic devices.

Substrate topography, coating and chemical composition at different scales may exert a dramatic effect on substrate wettability and on the liquid spreading dynamics. The observed behavior types of liquids on topographically or chemically textured substrates ranges from superhydrophobicity/superomniphobicity to superhydrophilicity and imbibition. These phenomena have been extensively discussed in literature (e.g. Cassie and Baxter 1944, Wenzel 1936, Bico et al. 2001, Boreyko et al. 2011, Butt et al. 2014, E5¹).

Many materials and elements of porous substrates are deformable. This includes rubber, gels, biological tissues as well as materials containing slender rods and sheets. The material deformability significantly affects the wettability as well as transport and phase change processes (Lester 1961, Rusanov 1975, Shanahan 1987, Sokuler et al. 2010, Lopes and Bonaccurso 2012, Alizadeh et al. 2013, Howland et al. 2016). The phenomena associated with elastocapillarity and findings in this rapidly developing field have been reviewed by Roman and Bico (2010), Style et al. (2017), Bico et al. (2018) and Chen et al. (2018).

Spreading of liquids on deformable substrates exerting capillary action or imbibition introduce a spectrum of new phenomena, including deviation from classical imbibition dynamics (Cambau et al. 2011), collapse of microchannels (Tanaka et al. 1993) and capillarity-driven assembly of fibers or filaments (Kang et al. 2010).

1.1.1 Liquid spreading, imbibition and evaporation on structured and porous substrates

In this project, we focus on structured and porous substrates promoting the spreading and lateral imbibition of liquids (Fig. 1). An overview of the state of the art on this topic can be found in (E5).

According to Bico et al. (2001), imbibition takes place if the material contact angle is below a critical contact angle θ_c :

$$\cos\theta_c = (1 - \phi_s)/(\phi_s - r_s). \quad (1)$$

Herein r_s denotes the substrate roughness, which is a ratio of the actual surface area to the projected area of the rough/microstructured substrate, and ϕ_s denotes the ratio of the solid area remaining dry (for example, the top surface of the micropillars) to the projected area. Therefore, the critical contact angle for imbibition is always below 90°. A substrate coated with a porous layer can be considered as a limiting case of a rough/microstructured substrate with the roughness r_s approaching infinity, leading to $\theta_c = 90^\circ$. The relation (1) does not contain information about the details of the substrate morphology. In contrast, Semprebon et al. (2014) analyzed the energy landscapes for different wetting states to predict the spontaneous imbibition criteria for defined microstructures comprised of arrays of pillars with circular or square cross-section.

The drop spreading and imbibition have been studied for a wide range of systems liquid/substrate, including pure liquids, surfactant solutions and complex liquids (such as blood) on filter paper (Starov et al. 2003, Trybala and Starov 2018) and pure liquids on substrates with defined structures (Courbin et al. 2009, Semprebon et al. 2014, Mekhitarian et al. 2017). In the most of the published works the main outcome of experimental observations is the evolution of the drop base radius (the radius at the contact with the substrate), the evolution of size (and shape) of the wetted region of the porous

¹ See Section 1.3. for the list of the project-related publications of the applicant

medium and the evolution of apparent contact angle at the droplet base. The typical drop behavior on porous layers in the cases where evaporation is not significant can be subdivided into three phases: (i) initial, relatively fast drop expansion, (ii) pinning of the contact line at the maximum reached spreading diameter and the decreasing of apparent contact angle due to the volume loss in the drop caused by the imbibition, and (iii) the shrinkage of the drop base at almost constant apparent receding contact angle accompanied by the further increasing of the imbibed area (Starov et al. 2003). In some systems the pinning phase does not take place. If evaporation is important, a final phase is added characterized by shrinkage of the imbibed area due to evaporation mass loss (see also section 1.2.1). The drop spreading and imbibition over substrates with defined structures (typically microscale posts arrays) follow a similar scenario, but show additional features, such as dependence of imbibition rate on direction, resulting in development of imbibed regions of different polygonal shapes (Courbin et al. 2009). Recently, an experimental work on spreading and evaporation of drops of highly volatile hydrofluoroether HFE-7100 over substrates composed of arrays of cylindrical SU-8 micropillars revealed the existence of different dynamic regimes, characterized by dominance of spreading/imbibition or evaporation. These regimes can be switched by changing the geometric parameters of the pillars array.

Theoretical/numerical models for description of drop spreading, imbibition and evaporation are typically based on Darcy-type flow within the porous layer or substrate microstructure. It is assumed that the flow in the layer is governed by capillary and viscous forces. In the regimes where the imbibition process is dominant, these models predict the \sqrt{t} – imbibition dynamics over a certain time interval, which is characteristic for Washburn-Lucas law (Washburn 1921). Application of Darcy-type flow models requires the knowledge of effective capillary pressure and permeability, which are determined by the geometrical parameters and wettability of the structured/porous layer.

In the cases where porous layers had a complex and not well defined structure, the combination of these two parameters have been extracted from the experiments on imbibition into a standing porous filter paper or membrane (Starov et al. 2003). In the case of defined microstructure approximate methods are often used to extract the imbibition model parameters (Bico et al. 2001, Mekhitarian et al. 2017). The models of liquid spreading/imbibition into the porous/structured layer are usually coupled with models of drop spreading over this layer (Starov et al. 2003, Mekhitarian et al. 2017) and evaporation.

Recently, the Computational Fluid Dynamics methods have been applied for direct numerical simulation of liquid imbibition into structural elements. Thammanna Gurumurthy et al. (2018a, b) have used Volume-of-Fluid (VoF) method for simulation of spontaneous propagation of a rivulet into a vertical corner. The influence of gravity has been taken into account. The results of simulations have confirmed the $t^{1/3}$ asymptotic for the capillary rise under gravity. This asymptotic law has been observed experimentally and predicted using a slender rivulet model, which allowed a similarity solution. The advantage of the direct CFD simulations is that they enable the analysis of flow beyond the validity limits of the simplifying assumptions underlying approximate solutions, i.e. the inertial effect and the real meniscus shape are automatically accounted for. However, the full-scale VoF simulations of drop spreading, imbibition and evaporation over porous/structured substrate require enormous time and computational resource and are therefore not realizable for practical purposes.

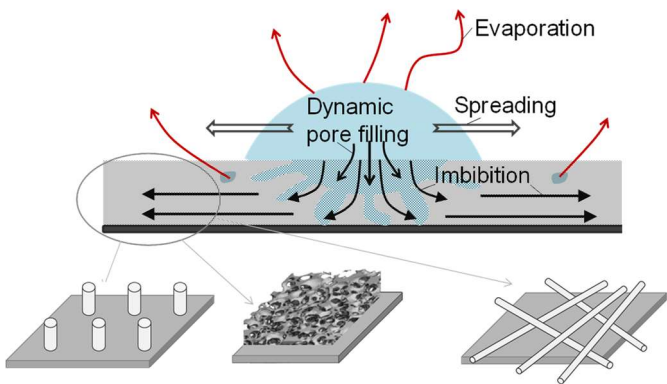


Figure 1: Schematic representation of drop spreading, imbibition and evaporation from structured or porous substrates.

1.1.2 Wetting of deformable substrates

Soft substrates are deformed in the vicinity of the contact line of sessile drops (Lester 1961, Shanahan 1987, Shanahan and Carré 2002). In addition, the equilibrium contact angle is modified on soft substrates in comparison with the value measured on a rigid substrate, and the drop spreading dynamics is governed by the mechanical properties of the solid. The reason of the substrate deformation is the normal component of the liquid surface tension acting at the contact line, $\sigma \sin\theta$, where σ denotes the surface tension and θ is the contact angle (Lester 1961, Rusanov 1975). At equilibrium this force leads to development of a stress field in the solid. The resulting deformation is scaled as $\sigma \sin\theta/E$, where E denotes the Young's modulus of the elastic solid. This deformation can amount to tens of micrometers for polymer gels and biological tissues.

Numerous theoretical and numerical works aimed at prediction of substrate deformation field are based on the theory of elasticity (Lester 1961, Rusanov 1975, White 2003, Marchand et al. 2012). The deformation is computed from the prescribed surface traction distribution on the surface of the elastic body. The deformation of the substrate and the angles formed between the phase interfaces strongly depend on the width of the area around the contact line, in which the upward stress is distributed (Lester 1961, Rusanov 1975, Lubbers et al. 2014). This width, a , which is associated with the capillary layer thickness in (Lester 1961) and referred to as molecular scale in (Marchand et al. 2012), cannot be determined from a macroscopic model. In the molecular dynamic simulations (Weijs et al. 2013), the width of the region around the contact line over which the stress is distributed is mostly determined by the parameters of the Lennard-Jones interaction potential. If the concept of disjoining pressure is used for description of intermolecular forces and their influence on the phenomena taking place near the contact line (Deryagin et al. 1982, White 2003, Kumar and Matar 2004, Ahmed et al. 2017, 2018, Koursari et al. 2018), the functional form of the disjoining pressure determines the area over which the stress is spread.

The most of the works mentioned above describe the equilibrium shape of the deformed substrate and of the liquid-gas interface. Ahmed et al. (2018) predict in addition the influence of substrate deformability on the contact angle hysteresis. However, in their work the modelling approach for computation of deformation field in the deformable substrate is oversimplified. Kumar and Matar (2004) use the long-wave theory (LWT, Oron et al. 1997) to describe the dynamic dewetting of liquid films on thin viscoelastic layers. To the best of the applicant's knowledge, no one of the existing numerical models can be used in the present form for description of dynamic spreading and evaporation of a drop over a deformable substrate with topography.

1.1.3 Elastocapillarity and imbibition

The capillary forces tend to bend slender structures such as thin sheets and rods (Roman and Bico 2010, Duprat and Protiere 2015, Bico et al. 2004, 2018). It has been estimated that a rod of diameter d should buckle if its length exceeds the critical value, $\sqrt{Ed^3/64\sigma}$ (Cohen and Mahadevan 2003). The bending leads to coalescence of elastic objects, which significantly affects the morphology of liquid wetting these objects (Duprat et al. 2012) and the dynamics of liquid imbibition between these objects, for example, between two flexible sheets (Duprat et al. 2011, Aristoff et al. 2011).

Evaporation affects the aggregation behavior of slender deformable objects and is in turn influenced by this aggregation. The mechanisms of this mutual influence are studied by Duprat et al. (2013), who investigated the diffusion-controlled evaporation of droplets on two parallel rigid and elastic fibers. Generally, the droplets in the column wetting state evaporate much faster than the droplets in the barrel wetting state, due to a higher area of the liquid-gas interface. It has been found for the rigid fibers that in the barrel (droplet) wetting state the evaporation rate is independent from the distance between the fibers, whereas for the column wetting state the evaporation rate increases with decreasing of the ratio between the interfiber distance and the fiber radius. If the fibers are elastic, the wetting state and evaporation rate are influenced by the deformation of fibers. Interestingly, even if the initial wetting state is the barrel state, evaporation can lead to the transition to the column state. This effect may lead to faster evaporation of liquid from fibrous media made of flexible material in comparison with the fibrous media made of rigid material.

Theoretical and numerical models for description of imbibition and evaporation of liquids in porous systems containing slender objects (such as fibers) are very rare. Some of them are aimed at

determination of equilibrium configurations of liquid volumes (Duprat et al. 2011, 2012), others are devoted to the prediction of liquid imbibition dynamics in simple configurations (e.g. between parallel flexible sheets) and under simplifying assumptions about the flow field (Aristoff et al. 2011). Simulations of elastocapillary coalescence of a large number of objects have been reported for the case of parallel flexible sheets modelled as spring-block elements, whereas the flow of liquid between them has been simulated using the lubrication theory (Singh et al. 2014, Hadjitoftis et al. 2016).

1.2 Preliminary work

The research at Institute of Technical Thermodynamics (TTD), TU Darmstadt, is focused on heat transfer and phase change in near-wall multiphase flows. The applicant heads a research group "Interfacial transport and complex wetting phenomena" and uses together with her group members theoretical, numerical and experimental tools for studying the hydrodynamics and transport phenomena in liquid films and drops as well as in the vicinity of three-phase contact lines.

1.2.1 Imbibition and evaporation of liquids on substrates with porous coatings

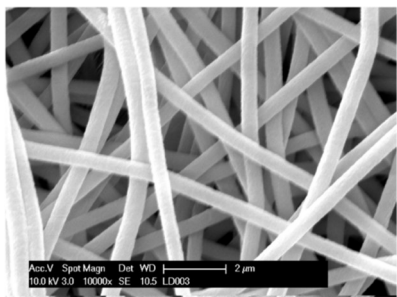


Figure 2: Scanning electron microscope image of PAN nanofibers.

The applicant has a long-term experience in investigation of wetting-driven flow, heat transfer and evaporation of liquids on substrates coated by nanofiber mats (Fig. 2). These mats are characterized by high porosity (around 90-95%), and their thickness varies typically (depending on the fabrication routine) from several tens of micrometers to around 1.5 mm. The most of experiments have been performed with nanomats produced from PAN [poly(acrylonitrile)], a partially wettable polymer with a water contact angle on a cast sample of about 30 - 40 °. The investigations have been performed in cooperation with Prof. A. Yarin (University of Illinois and Chicago).

It has been observed that the impact of cold droplet onto a hot stainless steel surface lead to stronger cooling effect in the case if the surface was covered by polymer nanofibers produced by electrospinning process (Srikanth et al. 2009). In addition, the cooling effect on the coated substrate was substantial at least at a distance of 1 cm from the impact point, whereas no cooling has been registered at this distance for a bare steel surface. These findings motivated further, detailed investigations of phenomena accompanying drop impact, spreading and evaporation onto nanofiber mat-coated unheated and heated substrates, which have been performed with involvement of TTD and Institute of Fluid Mechanics and Aerodynamics (SLA), TU Darmstadt (E9, E10, Weickgenannt et al. 2011b). It has been found that nanofiber mats suppress the drop splash (E9) and Leidenfrost phenomenon (Weickgenannt et al. 2011b), in this way increasing the amount of liquid in a direct contact with the substrate. In addition, it has been observed that, as soon as the liquid penetrates into the nanofiber mat, a lateral imbibition into the coating starts immediately, so that the maximum imbibition diameter reaches, depending on the properties of the nanomat and on thermodynamic conditions (substrate temperature, ambient humidity), up to 15-fold of the drop diameter before impact. After reaching the maximum diameter the impregnated region shrinks due to evaporation and eventually disappears completely.

The optical image of a heated nanomat-coated stainless steel foil taken from above 13 s after a water drop impact (Fig. 3a, left) reveals an imbibed area appearing as a dark region of diameter d_i . The infrared image of the back side of the foil at the same time instant (Fig. 3a, right) shows a circle of diameter d_i possessing a relatively uniform temperature distribution, corresponding to the area of intensive cooling. It has been shown that during the whole imbibition-evaporation cycle the values d_i and d_e were very close to each other. This indicates that the cooling of the substrate takes place predominantly by evaporation of the imbibed liquid. The evolution of the spreading (imbibition) diameter for different initial foil temperatures is depicted in Fig. 3b. The initial imbibition phase (increase of spreading diameter with time) is nearly independent from the foil temperature, indicating that the evaporation is insignificant at this time scale. As evaporation starts playing an important role, the evolution of spreading diameter slows down until the maximal spreading diameter, depending on the temperature, is reached. For lower temperatures, the imbibed area diameter stays constant

at the maximal level for a certain time interval, which can be explained by the balance between the imbibition and evaporation processes. We suggest that this balance would result in a steady state with a non-moving imbibition front in the case of infinite source of liquid. Since the total liquid volume over and inside the nanofiber mat is equal to the initial drop volume, the last phase of the cycle follows, which is governed by evaporation. During this phase the spreading/imbibition diameter decreases monotonically until the imbibed liquid evaporates completely.

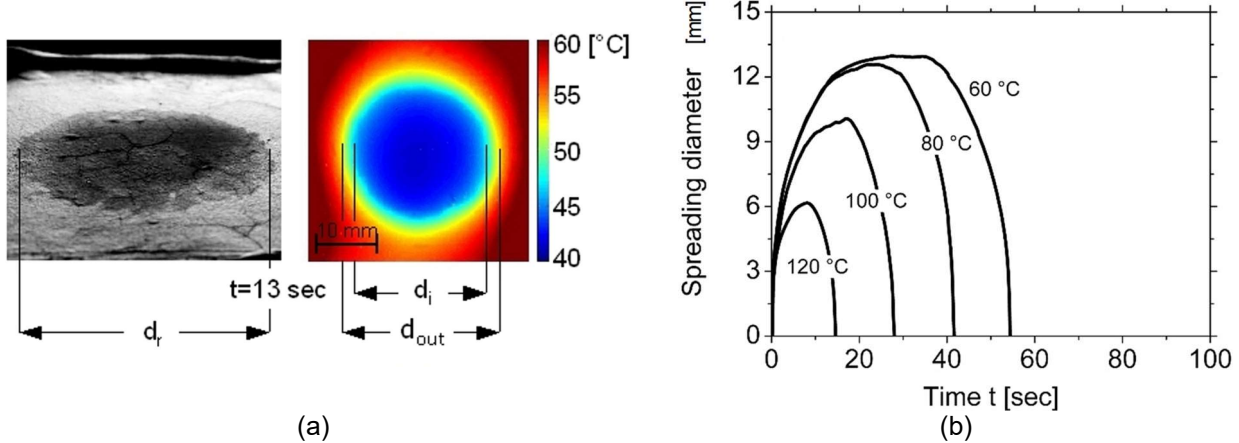


Figure 3: (a) Left: an optical image of a nanomat-coated heated steel foil (initial temperature: 60°C) from above, where the dark region of diameter d_r corresponds to the area impregnated by water 13 s after the drop impact. Right: an infrared image of the back side of the nanomat-heated steel foil under the drop impact location at the same time instant. The diameter d_i corresponds to the most intensively cooled area. (b) Spreading diameter versus time for different initial foil temperatures (E10).

The influence of nanofiber coatings on transport phenomena in flow boiling in minichannels has been studied using high speed infrared thermography and high speed black/white visualization of trains of Taylor bubbles (Freystein et al. 2016). The experiments have been performed with the fluorinert liquid FC-72. The heated wall of the minichannel has been covered by periodically arranged patches of nanomats, in which liquid was retained and thus kept in a permanent contact with the wall as the Taylor bubbles passed by. The evaporation of the retained liquid contributed significantly to the enhancement of heat removal from the heated wall. It has been found that the heat transfer coefficient at nanofiber mat-coated domains was an order of magnitude higher than that at the uncoated domains.

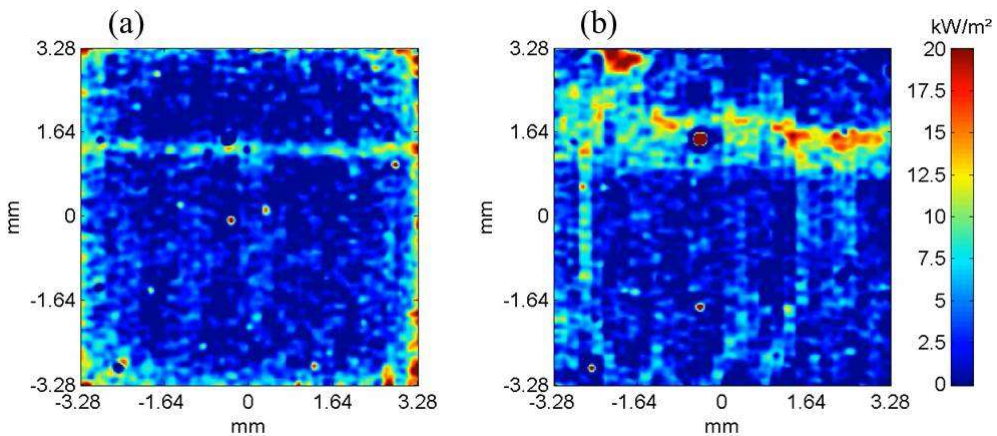


Figure 4: The fields of wall heat flux in the vicinity of the receding macroscopic receding meniscus (E4). (a) Uncoated substrate; (b) substrate coated with PAN nanofiber mat. The meniscus receding velocity in both cases is 10 mm/s. The test fluid is FC-72, the saturation temperature is 53 °C.

To understand the mechanisms of static and dynamic wetting and evaporation from substrates with nanoporous coatings, a series of experiments has been performed in a capillary gap with one heated side, in which a single static, advancing or receding macroscopic meniscus has been created (E4). The temperature at the wall-fluid interface has been registered using a high-speed infrared camera.

The instationary temperature fields have been used to compute the fields of wall heat flux distribution. The examples of heat flux distribution for receding meniscus are shown in Fig. 4 for uncoated (a) and nanomat-coated (b) heated wall. The thin straight line of high heat flux in Fig. 4a corresponds to the immediate vicinity of apparent three-phase contact line, where the local thickness of the liquid layer is very thin and, therefore, the thermal resistance to evaporation very low. For the heated wall coated with nanofiber mat (Fig. 4b) the region of elevated heat flux extends to the width of around 1 mm. This happens because the receding meniscus leaves behind a region of thin nanoporous coating containing evaporating liquid. This evaporation of liquid from multiple microscale and nanoscale menisci results in an extended high heat flux region. This mechanism is suggested to be responsible for heat transfer enhancement reached by application of nanofiber mat coatings in flow boiling experiment (Freystein et al. 2016).

Experimental investigation of liquid spreading, imbibition and evaporation on substrates with porous coatings are presently running under the supervision of applicant in the framework of DFG Collaborative Research Center (CRC) 1194 "Interaction between Transport and Wetting Processes".

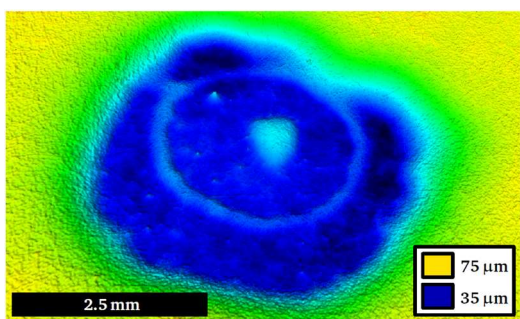


Figure 5: Deformation of nanofiber mat after evaporation of water drop.

The ongoing experiments have shown that, depending on the fluid, nanofiber mats may strongly deform due to wetting. An example of such deformations after the impact and evaporation of a water drop is shown in Fig. 5. As a substrate, a silicon wafer coated with a nanofiber mat was used. The topography was measured with a confocal microscope. The substrate has been coated at the Institute of Technical Thermodynamics using an electrospinning device (Avecetas Spraybase). The nanofiber mat was spun with a polymer solution of 5 wt% PAN (Polyacrylonitrile) and DMF (Dimethylformamide). The resulting fibers diameter was 200-300 nanometer, and the initial mat thickness was approximately 75 μm .

For the drop impact the distance of needle tip to substrate surface was set to 10 mm. The drop was of pure water with an initial diameter of 2.4 mm. After impact, the drop did not imbibe immediately into the coating, but stayed over the mat as a sessile drop with an apparent contact angle of around 90°. The substrate with the sessile drop was stored in a petri dish. After around 6 hours the drop was completely evaporated.

It is clearly seen that the drop spreading and evaporation resulted in a substantial deformation of the nanofiber mat, with the maximal difference between the highest and the lowest points on the mat surface of about 40 μm . The topography of the mat surface contains a thin elevation rim with diameter of approximately 2.5 mm. The contact line of the sessile drop was positioned on the location of this rim. After the most of the drop volume was evaporated and the apparent contact angle reached a certain critical value, the remaining liquid imbibed into the pores of the nanofiber mat, resulting in the outer valley that surrounds the inner rim. This experiment shows that the process of imbibition into the nanomat is accompanied by a strong elastocapillary deformation. It is suggested that the elastocapillary deformation significantly affects the rate of imbibition and evaporation.

Until now, no model exists which is able to describe and predict the imbibition and evaporation processes of liquids on deformable complex porous substrates. The development of such models are not ongoing and not planned within CRC 1194.

1.2.2 Theoretical, numerical and experimental studies of wetting of deformable substrates

Static and dynamic wetting of deformable substrates has been studied in the group of the applicant in the framework of EU Marie Curie Initial Training Network "Complex Wetting Phenomena" (CoWet), which has been coordinated by the applicant in the years 2014-2017.

Gielok et al. (E6) developed a model for description of a droplet wetting a deformable elastic substrate. A Finite Element Method (FEM) for solution of elasticity problem within the substrate has been coupled with lubrication approximation (or LWT) for modelling the droplet spreading. The axisymmetric system substrate-drop used in the model is schematically shown in Fig. 6. It is seen

that the film thickness beyond the apparent drop base radius is not zero. This is a very thin adsorbed film (thickness shown not to scale), which appears as result of the action of intermolecular forces. The action of intermolecular forces is described using the disjoining pressure concept. The form of the disjoining pressure used in (E6) and shown schematically in Fig. 7 describes the action of van der Waals interaction as well as the electrostatic and/or structural component (E1). This form allows determination of the adsorbed film thickness at the apparently dry substrate and of finite apparent contact angle using the Frumkin-Derjaguin equation (Frumkin 1938). In the model developed in (E6), the disjoining pressure and capillary pressure are used as a surface traction in the elasticity problem solved in the substrate. The resulting deformation of solid substrate (denoted as w in Fig. 6) is integrated into the long-wave drop evolution equation in the form of substrate topography. The coupling of two solutions takes place by an iterative procedure.

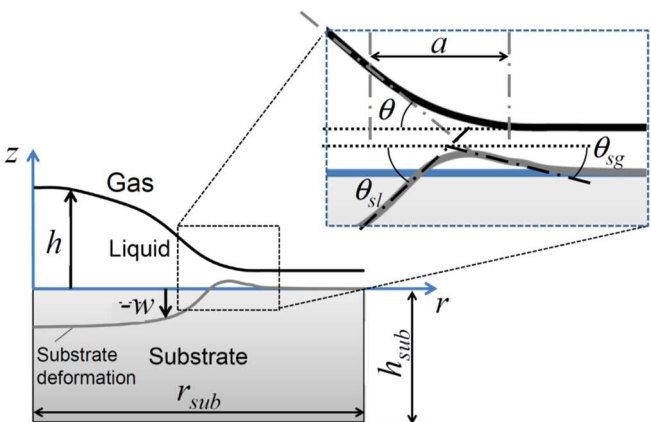


Figure 6: Scheme of the drop – substrate system for modelling static and dynamic wetting of elastic substrates (E6).

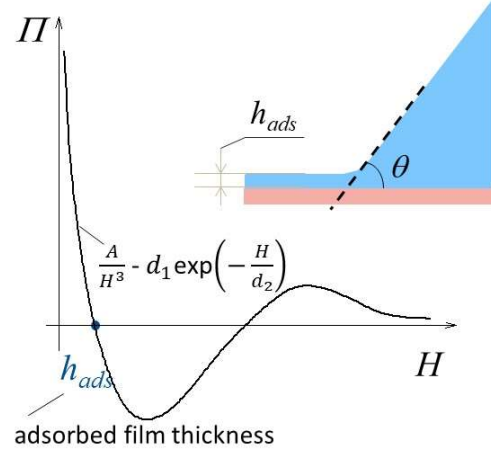


Figure 7: General form of the disjoining pressure (Π) dependence on the film thickness (H) used in (E6).

This modelling strategy has been applied to determination of the static sessile drop shape, the apparent contact angle (θ in Fig. 6), the substrate deformation and the solid angle formed due to this deformation ($\pi - \theta_{sl} - \theta_{sg}$ in Fig. 6) as functions of the elastic modulus of the substrate, the surface tension, the parameters of the disjoining pressure model and the substrate thickness. It has been found that the solid angle of the substrate deformation increases monotonously with increasing of the “microscale softness parameter”, $\sigma/(aE)$, in agreement with the results reported in Lubbers et al. (2014). The developed model can be applied to description of the drop spreading. Moreover, by adding terms describing phase change into the drop evolution equation, the model can be used for description of drop evaporation or condensation on deformable substrates (see Section 2.3).

The impact of viscous drops on deformable surfaces has been studied experimentally (E8). The soft substrates have been fabricated from polydimethylsiloxane (PDMS), whereas the mechanical properties of the substrates have been varied in a wide range by varying the ratio between the base polymer and the cross-linking agent. Water and water-glycerin mixtures have been chosen as test liquids, thus ensuring a strong variation of dynamic viscosity and moderate variation of surface tension. The drop velocities and diameters have also been varied. As a result, the Reynolds and Weber numbers could be varied independently during the experiment. It has been found out that the mechanical properties of the substrate have only a weak effect on the spreading of drop after the impact, but significantly influence the receding rate. Namely, the soft substrates lead to slowing down the drop receding rate, and the final drop contact diameter increases with increasing of the substrate softness, which is in agreement with the results reported in literature (Alizadeh et al. 2013). In addition, the suppression of drop splashing also reported previously (Howland et al. 2016) has been described in terms of splashing threshold line in the Weber-Reynolds-map.

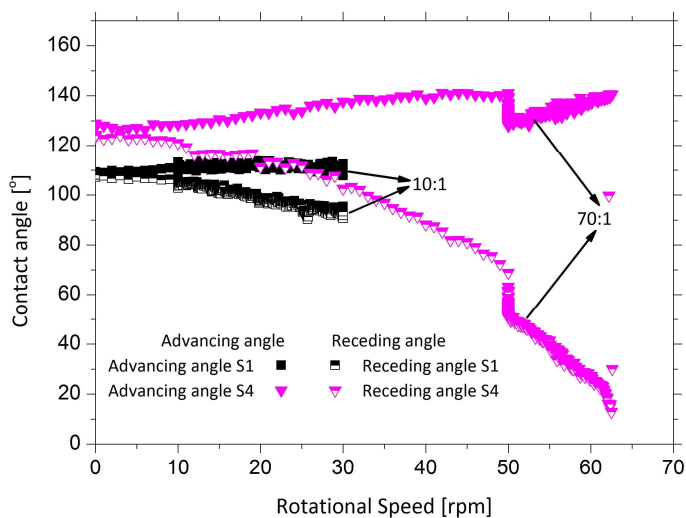


Figure 8: Advancing and receding contact angles of deformed water sessile drops on PDMS substrates with the mixing ratios polymer:cross-linking agent 10:1 (S1, shear modulus 703.4 kPa at 1 Hz) and 70:1 (S4, shear modulus 1.14 kPa at 1 Hz) as functions of the rotating speed. The distance from the position of the sessile drop to the rotation axis was 25 cm.

In cooperation with the group of Prof. T. Karapansios (Aristotle University of Thessaloniki) the influence of the substrate mechanical properties on the deformation and onset of sliding of a sessile drop under increasing centrifugal force has been studied. The dependence of the contact angle at the advancing and the receding edges of the droplet in the direction of the applied force, the drop length and the drop contour shape on the rotational speed has been analyzed. PDMS substrates at different mixing ratios between the polymer and the cross-linking agent have been used. Water and 50 wt% glycerin solution were chosen as the wetting liquids. Drops on softer surfaces showed a significantly larger hysteresis as compared to drops on the harder substrates (Fig. 8).

1.2.3 Theoretical and numerical studies of interfacial flows, wetting, transport phenomena and phase change

TTD and the research group of the applicant have a long-year experience in theoretical and numerical investigations of near-wall interfacial flows, wetting, heat and mass transport and phase change. The systems under study include liquid films and rivulets flowing under the action of gravity, gas flow and Marangoni stresses as well as drops impacting and spreading on hot walls and evaporating sessile drops. The influence of substrate topography and nonuniform thermal properties on evaporation and transport processes has been one of the research focuses of the group.

For description of film flows with small ratio between the characteristic film thickness and characteristic wave length of film thickness variation, the lubrication approximation, or LWT, has been used in the group of the applicant. With the help of this method, it has been predicted that longitudinal grooves arranged parallel to the flow direction suppress the waves on the surface of falling films (Gambaryan-Roisman and Stephan 2003). Using the same technique, it has been predicted that wall topography on heated substrates induces controlled Marangoni convection, interface deformation and film rupture at controlled locations (Gambaryan-Roisman et al. 2005, Kabova et al. 2006). Recently, the LWT-simulations have been extended to evaporating film on substrates with topography (E3).

Two-phase flows including evaporation in the vicinity of the apparent contact line have been described at TTD using a modular modelling strategy, which has been introduced by Stephan and Busse (1992). The challenge of description of such flows is caused by the very small size of the wall region (less than 1 μm in length) accounting for a significant portion of the total evaporation rate in the system (around 50% of the total evaporation rate from a sessile drop with diameter of around 1 mm). A micro scale description of processes taking place within the tiny region surrounding the apparent contact line ("micro region") is at the same time crucial for an accurate prediction of the heat and mass transport in the macroscopic system. In the modular modelling concept, the interface shape, flow and temperature field within the micro region are computed using the lubrication approximation, taking into account the action of intermolecular forces (in the form of disjoining pressure) and the deviation from equilibrium at the liquid-vapor interface. The micro region model yields the total heat flow per unit contact line length and the apparent contact angle as functions of the local wall temperature, contact line speed and thermodynamic conditions. These data are fed into the macroscopic numerical model describing the chosen system in form of correlations.

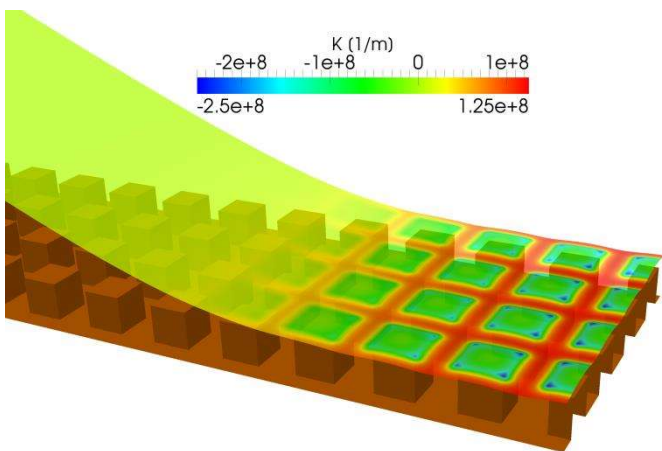


Figure 9: Shape of the liquid-vapor interface in the micro region on a nano-structured wall colored by curvature (E2).

The modular modelling strategy has been used in combination with FEM for description of heat transfer enhancement in evaporating falling films by using structured wall surfaces (Gambaryan-Roisman and Stephan 2003) and in combination with VoF method for simulation of drop impact, spreading, receding and evaporation on heated walls (E7, Herbert et al. 2013b). The micro region model has been originally developed for perfectly wetting liquids on smooth substrates. Later it has been extended to partially wetting liquids using the form of disjoining pressure illustrated in Fig. 7 (E1) and to substrates with nanoscale topography (E2, Fig. 9).

It can be concluded that understanding of spreading, imbibition and evaporation of drops on structured or porous deformable substrates is very important for further development of industrial processes, including ink-jet printing, needless injection, coating of porous materials, manufacturing of microfluidic devices and cooling technologies for high power electronic devices. This understanding can be achieved only by development of comprehensive theoretical and numerical models, taking into account the relevant physical processes taking place at different time and length scales.

1.3 List of project-related publications

1.3.1 Articles which at the time of proposal submission have been published or officially accepted by publication outlets with scientific quality assurance

- E1 Ajaev, V.S., Gambaryan-Roisman, T., Stephan, P., Static and dynamic contact angles of evaporating liquids on heated surfaces, *J. Colloid Interface Sci.* 342 (2010), 550-558
- E2 Batzdorf, S., Gambaryan-Roisman, T., Stephan, P., Direct numerical simulation of the heat and mass transfer in the 3-phase contact line region, *ASME J. Heat Transfer* 140 (2018), 032401
- E3 Bender, A., Stephan, P., Gambaryan-Roisman, T., Numerical investigation of the evolution and breakup of an evaporating liquid film on a structured wall, *Int. J. Heat Fluid Flow* 70 (2018), 104-113
- E4 Fischer, S., Sahu, R.P., Sinha-Ray, S., Yarin, A.L., Gambaryan-Roisman, T., Stephan P., Effect of nano-textured heater surfaces on evaporation at a single meniscus, *Int. J. Heat Mass Transf.* 108 (2017), 2444-2450
- E5 Gambaryan-Roisman, T., Liquids on porous layers: Wetting, imbibition and transport processes, *Curr. Opin. Colloid Interface Sci.* 19 (2014), 320-335
- E6 Gielok, M., Lopes, M., Bonacurso, E., Gambaryan-Roisman, T., Droplet on an elastic substrate: Finite Element Method coupled with lubrication approximation, *Colloids Surf. A* 521 (2017), 13-21
- E7 Herbert, S., Fischer, S., Gambaryan-Roisman, T., Stephan, P., Local heat transfer and phase change phenomena during single drop impingement on a hot surface, *Int. J. Heat Mass Transfer* 61 (2013a), 605-614
- E8 Kittel, H.M., Alam, E., Roisman, I.V., Tropea, C., Gambaryan-Roisman, T., Splashing of a Newtonian drop impacted onto a solid substrate coated by a thin soft layer, *Colloids Surf. A* 553 (2018), 89-96
- E9 Lembach, A.N., Tan, H.-B., Roisman, I.V., Gambaryan-Roisman, T., Zhang, Y., Tropea, C., Yarin, A.L., Drop impact, spreading, splashing and penetration into electrospun nanofiber mats, *Langmuir* 26 (2009), 9516-9523
- E10 Weickgenannt, C.M., Zhang, Y., Lembach, A. N., Roisman, I.V., Gambaryan-Roisman, T., Yarin, A.L., Tropea, C., Non-isothermal drop impact and evaporation on polymer nanofiber mats, *Phys. Rev. E* 83 (2011a), 036305

1.3.2 Other publications

Not applicable

2 Objectives and work programme

2.1 Anticipated total duration of the project

The intended project duration is 36 months. The DFG funds will be necessary for the entire duration. The anticipated starting date of the project is 01.10.2019.

2.2 Objectives

The planned project is aimed at development and validation of theoretical and numerical models for spreading, imbibition and evaporation of liquids on structured or porous substrates, taking into account the deformability of the substrate and of elements of the porous structure. The models will facilitate understanding of the influence of the substrate structure, the mechanical and surface properties of the material, the properties of the liquid, the thermodynamic conditions and configuration on the wetting dynamics as well as heat and mass transfer. The numerical models will be implemented in codes which will be shared within the scientific community. Simulations will be performed to gain understanding of the influence of governing parameters (physical properties and structure of the substrate, properties of wetting liquid, thermodynamic conditions) on dynamics of spreading, imbibition, transport processes and evaporation.

In the first three-year term, the numerical model will be developed, validated and applied to a special limited class of substrate structures, whereas the full understanding of the material, structural and process parameters on spreading, imbibition and evaporation process will be achieved. At the same time, the preparations for modelling of more complex structured and porous substrates will take place. Namely, the wetting and evaporation of liquid on grooves and fibers and groups of fibers will allow to elucidate the key phenomena governing the imbibition on a larger scale.

In the second three-year term, on the basis of the knowledge gained in the first phase, a framework for description of global imbibition and evaporation on surfaces with several classes of topography relevant to natural phenomena and technological applications will be developed. These classes will include substrates with grooves with height-to-width aspect ratio of order of unity and higher as well as substrates coated with nanofiber mats. Homogenization techniques will be used for computation of effective transport coefficients. These coefficients will be further used for microscopic-scale simulation of imbibition and evaporation processes.

The global objective for the first three-year term will be achieved in several steps, for which the following specific goals are defined:

G1 Development of a model describing the drop spreading and evaporation on smooth deformable substrates

Since the process under study is governed by several coupled physical phenomena, this step is necessary to get an understanding of the influence of material and process parameters on the time and length scales at which different phenomena are dominant.

G2 Development of a model describing drop spreading and evaporation on deformable substrates with a shallow topography

This step is necessary for determination of the influence of the geometric parameters of the structured substrate on the dynamics of the involved processes. It should be noted that at this step a limited class of substrate topographies can be described. Some of the questions to be answered are:

- At which conditions the spreading of drop over a substrate with topography can be described as a combination of drop spreading over the substrate structure and liquid imbibition into the structure?
- How the combination of substrate structure and deformability influences the contact angle hysteresis?

G3 Development of a model describing the local phenomena in the vicinity of the three-phase contact line

The vision is to create a framework which enables modelling of the dynamic wetting and evaporation phenomena on deformable substrates in different configurations. In many cases the scale at which the strong substrate deformation and strong evaporation rates are developed is much smaller than the problem-specific macroscopic scales. In these cases, the separation of scales can be employed, and the local substrate deformation, liquid-gas interface shape and evaporation rate in the vicinity of the apparent contact line can be modelled independently from the global configuration. These results can be implemented as subgrid models for large scale simulations of wetting dynamics.

G4 Development of models describing wetting and evaporation on elements of porous substrates

Towards description of imbibition into deformable substrates and porous coating of industrial relevance (beyond the limitations shallow topography), the wetting and evaporation on typical elements of topography or elements of porous substrates (corners, fibers) should be modelled numerically.

G5 Development of a model describing liquid imbibition and evaporation on a group of fibers

This specific process strongly coupled with the coalescence of fibers is important for understanding of imbibition and evaporation on substrates with nanofiber coatings and for many additional systems and applications, including textiles, filters and fibrils.

G6 Experimental validation of the drop spreading, imbibition and evaporation models

While numerous experimental data are available and are presently being collected (e.g. in the framework of CRC 1194) for validation of the future global model of drop spreading, imbibition and evaporation on substrates with deformable porous coatings, the validation data for the results of preliminary modelling steps are unavailable and should be collected in the framework of this project.

In the following work programme the work steps towards the achievement of the above specific goals are described in details in corresponding Work Packages (WP).

2.3 Work programme including proposed research methods

The research methods planned in this project are based on the previous experience of the applicant and TTD. They include the LWT-simulations combined with FEM for solution of elasticity problem in the substrate and semi-analytical description of vapor diffusion in the gas phase; FEM for simulation of local phenomena in the vicinity of the contact line beyond the validity of LWT, and using applying modular strategy for simulation of wetting of elements of porous structure. For the validation experiments, the established experimental techniques, setups and analysis techniques will be used.

2.3.1 Time plan and work packages (WPs)

The WPs described below are designed for achievement of specific goals defined in Section 2.2.

WP 1 Drop spreading and evaporation on smooth deformable substrates

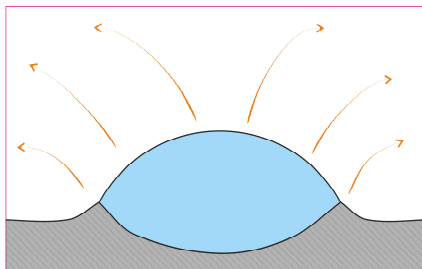


Figure 10: Schematic representation of configuration to be modelled in WP 1.

The configuration to be modelled is schematically presented in Fig. 10. The model is based on solution of axisymmetric LWT for description of drop evaporation combined with FEM in the elastic substrate, the approach which has been applied in (E6). This approach is applicable for situations where the assumption underlying the LWT is fulfilled: the characteristic film thickness is much smaller than the characteristic length scale of the film thickness variation, i.e. for thin drops.

The LWT evolution equation for the film thickness used in (E6) will be augmented by an additional term describing the evaporation mass loss:

$$H_t + \frac{j_{ev}}{\rho} + \frac{1}{3\mu} \left\{ H^3 r \left[\frac{\sigma}{r} h_r + \sigma h_{rr} + \Pi \right]_r \right\}_r = 0, \quad (2)$$

where μ and ρ denote the dynamic viscosity and density of the liquid, respectively, $H = h - w$ is the local film thickness, j_{ev} is the mass flux of liquid evaporation, $\Pi(H)$ is the disjoining pressure, which is the function of the local film thickness. The radial coordinate r , the position of liquid-gas interface h and the position of solid-fluid interface w are illustrated in Fig. 6. In WP 1, in the absence of drop the substrate is not deformed: $w=0$. The deformation of the substrate is a result of the action of surface traction in the form (White 2003, E6):

$$f(r) = \Pi(H) + \Delta P, \quad (3)$$

where ΔP denotes the Laplace pressure.

The expression for j_{ev} depends on the choice of thermodynamic conditions and the corresponding evaporation mode. If the evaporation takes place in pure vapor atmosphere and the substrate temperature is higher than the saturation temperature, the evaporation rate is limited by the local thermal resistance of the liquid layer and the interfacial thermal resistance. In addition, in the immediate vicinity of the apparent contact line, augmented Thomson equation should be taken into account. The expression for j_{ev} in this case can be found in (Stephan and Busse 1992, E1, E2). If the evaporation takes place in the presence of non-condensable gas, the evaporation rate is determined by the transport of vapor in the gas atmosphere. In this case the solution of vapor transport equation over the substrate should be solved simultaneously with the solution of evolution equation (2) and the elasticity problem in the substrate. It will be assumed that the free convection in the gas is negligible and that the vapor distribution in the gas can be described by the stationary diffusion equation. The integration of the evaporation rate into the drop evolution equation can be performed using an integral representation as in the work of Eggers and Pismen (2010). It has been found that, if the thermal conductivity and thermal effusivity of the substrate are low, the evaporation leads to significant cooling of the substrate. This effect, in turn, reduces the evaporation rate (Lopes et al. 2013). Therefore, the heat conduction equation within the substrate will be solved using FEM along with solution of elasticity problem for selected sets of parameters.

Presently, the evolution equation does not include the terms describing the effect of hydrostatic pressure, since it is assumed that the drop size is below the Bond number is small. However, this effect can be easily included in the future.

The governing dimensionless parameters of the spreading and evaporation process include, but are not limited to:

θ_{eq}	equilibrium contact angle on undeformed substrate
$\sigma/(Ed_{dr})$	parameter relating substrate deformation length scale to the volume-based drop diameter
$\sigma/(Ea)$	parameter relating substrate deformation length scale to the molecular scale associated with the region of action of disjoining pressure
$D\Delta cv/(\sigma d_{dr})$	parameter relating the diffusion-controlled evaporation rate to characteristic capillary velocity. Here v is the kinematic viscosity of the liquid, D is the diffusivity of the vapor in the gas phase and Δc is the characteristic difference between the saturation concentration of the vapor at the liquid-gas interface and the far-field vapor concentration
$\mu v/(\sigma d_{dr})$	parameter which can be related to Crispation number
h_{sub}/d_{dr}	relation between the substrate thickness and drop diameter

The simulations of drop spreading and evaporation in combination with solution of elasticity problem in the substrate will be performed for different combinations of parameters, corresponding to different substrates and liquids, different environmental conditions and the sizes of the substrate and the drop. For these simulations, a combined Matlab/COMSOL code developed at TTD will be used. In the framework of exchange with the project lead by U. Thiele (WWU Münster) the results of several reference simulation cases will be compared with the results of gradient dynamic modelling

approach. The simulation code will be made available to the participants of SPP. In cooperation with WWU Münster tutorials will be developed to facilitate the usage of the code.

The results of the simulations will be analyzed to extract the temporal evolution of the apparent spreading (contact) radius and apparent contact angle for different sets of governing dimensionless parameters.

In cooperation with E. Dörsam (TU Darmstadt) the lubrication model will be modified to apply to layer of ink on an elastic printing plate.

WP 2 Drop spreading and evaporation on deformable substrates with shallow topography

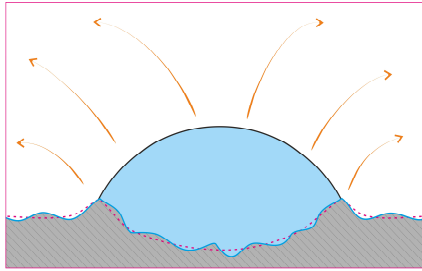


Figure 11: Schematic representation of configuration to be modelled in WP 2.

The evolution equation (2) will be re-written in a full two-dimensional form. In contrast to WP 1, the substrate deformation in the absence of drop is not zero (see Fig. 11). This deformation is defined by a function $w = w_0(x, y)$, where x and y are coordinate axes in the plane of the substrate-fluid interface. The LWT approach is applicable as soon as the characteristic wave length of the structure described by the function $w_0(x, y)$ is much larger than the characteristic film thickness. This means that the topography should be shallow. In WP 2, periodic structures will be typically used. These include parallel grooves and elevations arranged in square or hexagonal arrays.

In addition to governing dimensionless parameters listed in description of WP 1, the new parameters are introduced in WP 2, namely, the aspect ratio of the substrate topography elements as well as the ratio between the length scale of the topography element and the drop diameter. In the typical simulation runs, the topography length scale is significantly smaller than the drop diameter.

The simulations will be run to extract the size and shape evolution of the wetted zone. The combinations of parameters will be determined, for which typical imbibition-like wetting dynamics is predicted. For these cases, the effective permeability and effective capillary pressure of the structure will be extracted from the simulation results and related to the geometrical parameters of the structure. Another focus will be laid on determination of regimes, for which the wetted area has a circular or polygonal shape as observed in (Courbin et al. 2009, Mekhitarian et al. 2017). The evolution of the liquid-gas interface shape will be analyzed to determine the regimes for which the interface can be described as a spherical cap sitting on top of structure impregnated by liquid (Starov et al. 2003, Mekhitarian et al. 2017). For these regimes, the evolution of the spherical cap will be analyzed.

In the limiting case of rigid substrates with topography, the results of simulations will be validated by comparison with the results gained in the project of O. Varlamova/R. Borcia (BTU Cottbus-Senftenberg).

WP 3 Microscale model of local substrate deformation, liquid-gas interface shape and transport phenomena in the vicinity of evaporating contact line

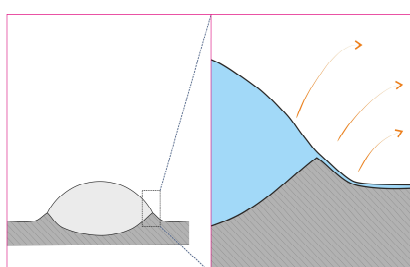


Figure 12: Schematic representation of the region in the vicinity of apparent three-phase contact line to be modelled in WP 3.

The shape of liquid-gas interface and deformation of the elastic solid will be considered in an immediate vicinity of the apparent three-phase contact line (Fig. 12, right). The system is assumed to be at a stationary state in the frame of reference fixed at the apparent contact line. Stationary contact line or contact line moving with a constant velocity (advancing or receding) will be modelled. The computational domain extends to the apparently dry substrate, which is covered by the adsorbed liquid film, and where the substrate deformation is relaxed to zero. At the side of the liquid wedge, the computational domain extends to the region where the curvature of the liquid-gas interface reduces to zero. At this point the apparent contact angle is determined.

The input parameters of the model include the material properties, the parameters of the disjoining pressure isotherm, the thermodynamic conditions and the contact line velocity. The output parameters are the apparent contact angle, the maximal height of the substrate deformation and the integral evaporation rate per unit contact line length. For low contact angles, LWT approach will be used (similar to WP 1). For higher contact angles (still below $\pi/2$), direct numerical simulations will be applied (see E2). The results of the simulations can be stored in the form of look-up tables or correlations and used later in subgrid models in different wetting configurations, similar to the micro region evaporation model which is established at TTD (Stephan and Busse 1992, Gambaryan-Roisman and Stephan 2003, E7).

The look-up tables/correlations will be made available to scientific community. They can be used by SPP members, for example, in the group of P. Huber (TUHH) for modelling the liquid imbibition into deformable pores.

WP 4 Wetting and evaporation of elements of porous substrates

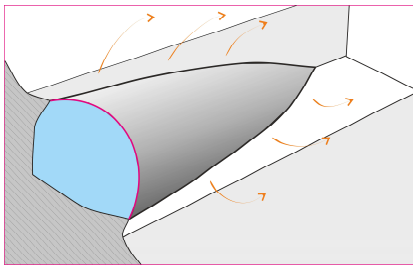


Figure 13: Schematic representation of liquid imbibition into a corner and simultaneous evaporation – one of configurations to be modelled in WP 4.

In this WP, the typical elements of substrate topography and porous structures, which could not be described in WP 2, will be considered. A typical reference configuration is a spontaneous imbibition of liquid into a corner manufactured of deformable material (Fig. 13). This problem will be solved using an approximation of a slender rivulet with unidirectional flow field. This model will be an extension of the slender rivulet approximation described in (Thammanna Gurumurthy et al. 2018), where the effect of evaporation will be added, and the results of the contact line model (WP 3) will be implemented.

As a second element, a fiber will be considered. Since one of the long-term project goals is development of a model for describing the imbibition into nanofiber mats, one of important questions to be clarified will be the influence of the nanofiber diameter, which is comparable with the length scale of action of long-range intermolecular forces (taken into account in the form of disjoining pressure), on the apparent contact angle, wetting and evaporation dynamics.

The results of the simulation of the contact line propagation along a single fiber will be provided to the group of M. Biesalski and T. Meckel (TU Darmstadt) for joint analysis.

WP 5 Imbibition and evaporation on groups of fibers

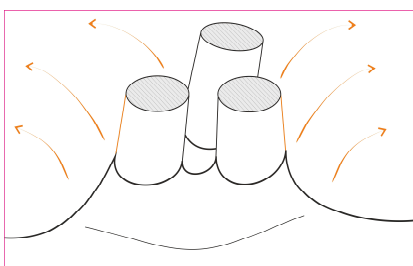


Figure 14: Schematic representation of liquid meniscus around a group of fibers – configuration to be modelled in WP 5.

This WP is devoted to investigation of mechanism of coalescence of flexible fibers under the action of capillary pressure and of the influence of coalescence on imbibition and evaporation. In contrast to elastocapillary imbibition between two parallel flexible sheets described in the literature (Aristoff et al. 2011), where the gap at the meniscus eventually reaches zero and the imbibition stops, the meniscus formed by coalescence of two or more fibers is never closed, and the dynamic of imbibition is therefore expected to significantly differ from that between the flexible sheets. Since the curvature of meniscus between the merged fibers has the same order of magnitude as that of the fiber itself, the fibers shape should be taken into account by developing the model of the imbibition and evaporation in a group of fibers after the merging.

The model describing dynamics of meniscus propagation between the fibers will be validated experimentally in collaboration with the project of M. Biesalski and T. Meckel (TU Darmstadt). In their project, the position of liquid-gas interface relative to single fibers will be visualized using confocal microscopy.

The magnetic microcolumns used in the project of J. Hussong/E. Gurevich (Ruhr-Universität Bochum) can stick together upon liquid evaporation. These experimental observations will be compared with the results of WP 5.

In addition, an interdisciplinary exchange with the project of C. Burkhardt (University of Tübingen)/ W. Konrad, C. Neinhuis, D. Voigt (TUD)/ A. Roth-Nebelsick (SMNS) studying liquid/gas interface at the flexible fibril membranes is possible.

WP 6 Experimental validation

The results of simulations performed in WP 1 and WP 2 will be experimentally validated in this WP. Two experimental cells available at TTD for investigation of drops spreading and evaporation are designed for pure vapor atmosphere and nitrogen atmosphere with controlled humidity, respectively. The typical drop diameter is around 1 mm. The evolution of the drop shapes during spreading will be recorded using high-speed B/W cameras equipped with telecentric lenses. The infrastructure and experience in manufacturing smooth deformable substrates with controllable mechanical properties are available (E8). The validation of the simulation results gained in WP 2 (deformable substrates with shallow topography) will be performed in cooperation with F. Müller (Friedrich-Schiller-Universität Jena) who will provide deformable polymer substrates with defined topography. In order to cover a wide range of dimensionless governing parameters, the variation of drop size in a wide range is advantageous. The experiments with spreading of micrometer-size drops will be performed in cooperation with R. Müller, H. Hasse, K. Langenbach and S. Antonyuk (TU Kaiserlautern) who possess a setup allowing creation of small sessile drops high-speed observation of three-dimensional drop evolution.

The experimentally observed evolution of drop shape and the size and shape of the wetted region will be compared with the results of simulations towards validation of numerical model.

Table 1: Time plan

Work Packages (WP)	2019					2020				2021				2022		
	Q4	Q1	Q2	Q3	Q4	Q1	Q2	Q3	Q4	Q1	Q2	Q3	Q4	Q1	Q2	Q3
1 Smooth deformable substrates																
2 Deformable substrates with shallow topography																
3 Contact line																
4 Elements of porous structure																
5 Groups of fibers																
6 Validation																

2.4 Data handling

The numerical codes and data generated in numerical simulations as well as the data collected in validation experiments will be saved and backups will be created. The TU Darmstadt follows the policy of making research data available for the public on a long-term standard. In addition to raw data, meta data are stored to enable a later reconstruction of project results.

The applicant is a participant of the CRC 1194, which contributes, together with the computing center of the TU Darmstadt and the University and federal library to the development of a concept for long-term usability and accessibility of research data. These concepts will be implemented into the information management facilities of the TU Darmstadt.

2.5 Other information

Not applicable

2.6 Explanations on the proposed investigations

In this project no experiments involving humans, human materials or animals will be performed. No immediate risk of yielding knowledge that could be intentionally misused has been identified.

2.7 Information on scientific and financial involvement of international cooperation partners

Not applicable

2.8 Information on scientific cooperation within SPP 2171

The planned scientific cooperation has been briefly described in the work programme. Below is the list of scientists, with whom the intended cooperation has been agreed upon.

- Prof. Dr.-Ing. E. Dörsam, TU Darmstadt
- Prof. Dr. rer. nat. Evgeny Gurevich, Jun.-Prof. Dr.- Ing. Jeanette Hussong, Ruhr-Universität Bochum
- Prof. Dr. rer. nat. Patrick Huber, TUHH
- Prof. Dr.-Ing. habil. Frank A. Müller, Friedrich-Schiller-Universität Jena
- Prof Dr.-Ing. Ralf Müller, Prof Dr.-Ing. Hans Hasse, Jun. Prof Dr.-Ing. Kai Langenbach and Prof Dr.-Ing. Sergiy Antonyuk, TU Kaiserslautern
- Prof. Dr. Uwe Thiele, WWU Münster
- Dr. Olga Varlamova/PD Dr. Rodica Borcia, BTU Cottbus-Senftenberg

3 Bibliography

- Ahmed, G., Kalinin, V.V., Arjmandi-Tash, O., Starov, V.M., Equilibrium of droplets on a deformable substrate: Influence of disjoining pressure, *Colloids Surf. A* 521 (2017), 3-12
- Ahmed, G., Koursari, N., Kuchin, I.V., Starov, V.M., Hysteresis of contact angle of sessile droplets on deformable substrates: Influence of disjoining pressure, *Colloids Surf. A* 546 (2018), 129-135
- Alizadeh A., Bahadur, V., Shang, W., Zhu, Y., Buckley, D., Dhinojwala, A., Sohal, M., Influence of substrate elasticity on droplet impact dynamics, *Langmuir* 29 (2013), 4520-4524
- Aristoff, J.M., Duprat, C., Stone, H.A., Elastocapillary imbibition, *Int. J. Non-Linear Mech.* 46 (2011), 648-656
- Bico, J., Tordeax, C., Quéré, D., Rough wetting, *Europhys. Lett.* 55 (2001), pp. 214-220
- Bico, J., Roman, B., Moulin, L., Boudaoud, A., Elastocapillary coalescence in wet hair, *Nature* 432 (2004), 690
- Bico, J., Reyssat, É., Roman, B., Elastocapillarity: when surface tension deforms elastic solids, *Annu. Rev. Fluid Mech.* 50 (2018), 629-659
- Boreyko, J.B., Baker, C.H., Poley, C.R., Chen, C.-H., Wetting and dewetting transitions on hierarchical superhydrophobic surfaces, *Langmuir* 27 (2011), 7502-7509
- Butt, H.-J., Roisman, I.V., Brinkmann, M., Papadopoulos, P., Vollmer, D., Semprebon, C., Characterization of super liquid-repellent surfaces, *Curr. Opin. Colloid Interface Sci.* 19 (2014), 343-354
- Cambau, T., Bico, J., Reyssat, E., Capillary rise between flexible walls, *EPL* 96 (2011), 24001
- Cassie, A.B.D., Baxter, S., Wettability of porous surfaces, *Trans. Faraday Soc.* 40 (1944), 0546-0550
- Chen, L., Bonaccurso, E., Gambaryan-Roisman, T., Starov, V., Koursari, N., Zhao, Y., Static and dynamic wetting of soft substrates, *Curr. Opin. Colloid Interface Sci.* 36 (2018), 46-57
- Cohen, A.E., Mahadevan, L., Kinks, rings, and rackets in filamentous structures, *PNAS* 100 (2003), 12141-12146
- Courbin, L., Bird, J.C., Reyssat, M., Stone, H.A., Dynamics of wetting: from inertial spreading to viscous imbibition, *J. Phys.: Condens. Matter* 21 (2009), 464127
- Deryagin, B., Starov, V., Churaev, N., Pressure on a wetting perimeter, *Colloid J. USSR* 44 (1982), 770-775
- Duprat , C., Aristoff, J.M., Stone, H.A., Dynamics of elastocapillary rise, *J. Fluid Mech.* 679 (2011), 641-654
- Duprat, C., Protière, S., Beebe, A.Y., Stone, H.A., Wetting of flexible fibre arrays, *Nature* 482 (2012), 510-513
- Duprat, C., Bick, A.D., Warren, P.B., Stone, H.A., Evaporation of drops on two parallel fibers: Influence of the liquid morphology and fiber elasticity, *Langmuir* 29 (2013), 7857-7863.
- Duprat, C., Protiere, S., Capillary stretching of fibers, *EPL* 111 (2015), 56006

- Eggers, J., Pismen, L., Nonlocal description of evaporating drops, *Phys. Fluids* 22 (2010), 112101
- Freystein, M., Kolberg, F., Spiegel, L., Sinha-Ray, S., Sahu, R.P., Yarin, A. L., Gambaryan-Roisman, T., Stephan P., Trains of Taylor bubbles over hot nano-textured mini-channel surface, *Int. J. Heat Mass Transf.* 93 (2016), 827-833
- Frumkin, A., On the phenomena of wetting and sticking of bubbles, *Zh. Fiz. Khim.* 12 (1938), 337-345
- Gambaryan-Roisman, T., Stephan, P., Analysis of falling film evaporation on grooved surfaces, *J. Enhanced Heat Transfer* 10 (2003), 445-457
- Gambaryan-Roisman, T., Alexeev, A., Stephan, P., Effect of the microscale wall topography on the thermocapillary convection within a heated liquid film, *Experimental Thermal and Fluid Science* 29 (2005), 765-772
- Hadjitofis, A., Lister, J.R., Singh, K., Vella, D., Evaporation effects in elastocapillary aggregation, *J. Fluid Mech.* 792 (2016), 168-185
- Herbert, S., Gambaryan-Roisman, T., Stephan, P., Influence of governing dimensionless parameters on heat transfer during single drop impingement onto a hot wall, *Colloids and Surfaces A: Physicochemical and Engineering Aspects* 432 (2013b), 57-63
- Howland, C.J., Antkowiak, A., Castrejón-Pita, J.R., Howison, S.D., Oliver, J.M., Style, R.W., Castrejón-Pita, A.A., It's harder to splash on soft solids, *Phys. Rev. Lett.* 117 (2016), 184502
- Kabova, Yu. O., Alexeev, A., Gambaryan-Roisman, T., Stephan, P., Marangoni-induced deformation and rupture of a liquid film on a heated microstructured wall, *Phys. Fluids* 18 (2006), 012104
- Kang, S.H., Pokroy, B., Mahadevan, L., Aizenberg, J., Control of shape and size of nanopillar assembly by adhesion-mediated elastocapillary interaction, *ASC Nano* 4 (2010), 6323-6331
- Koursari, N., Ahmed, G., Starov, V.M., Equilibrium droplets on deformable substrates: Equilibrium conditions, *Langmuir* 19 (2018), 5672-5677
- Kumar, S., Matar, O., Dewetting of thin liquid films near soft elastomeric layers, *J. Colloid Interface Sci.* 273 (2004), 581-588
- Lester, G.R. Contact angles of liquids at deformable solid surfaces, *J. Colloid Sci.* 16 (1961), 315-326
- Lopes, M., Bonaccurso, E., Evaporation control of sessile water drops by soft viscoelastic surfaces, *Soft Matter* 8 (2012), 7875-7881
- Lopes, M.C., Bonaccurso, E., Gambaryan-Roisman, T., Stephan, P., Influence of the substrate thermal properties on sessile droplet evaporation: Effect of transient heat transport, *Colloids Surf. A* 432 (2013), 64-70
- Lubbers, L., Weijs, J., Botto, L., Das, S., Andreotti, B., Snoeijer, J., Drops on soft solids: free energy and double transition of contact angles, *J. Fluid Mech.* 747 (2014), R1
- Marchand, A., Das, S., Snoeijer, J., Andreotti, B., Contact angles on a soft solid: from Young's law to Neumann's law, *Phys. Rev. Lett.* 109 (2012), 236101
- Mekhitarian, L., Sobac, B., Dehaek, S., Haut, B., Colinet, P., Evaporation dynamics of completely wetting drops on geometrically textured surfaces, *EPL* 120 (2017), 16001
- Oron, A., Davis, S., Bankoff, S., Long-scale evolution of thin liquid films, *Rev. Mod. Phys.* 69 (1997), 931-980
- Roman, B., Bico, J., Elasto-capillarity: deforming an elastic structure with a liquid droplet, *J. Phys. Condens. Matter* 22 (2010) 493101
- Rusanov, A.I., Theory of wetting of elastically deformed bodies.1. Deformation with a finite contact-angle, *Colloid J USSR* 37 (1975), 614-622
- Semprebon, C., Forstberg, P., Priest, C., Brinkmann, M., Pinning and wicking in regular pillar arrays, *Soft Matter* 10 (2014), 5739-5748
- Shanahan, M., The influence of solid micro-deformation on contact angle equilibrium, *J. Phys. D: Appl. Phys.* 2 (1987), 945-950
- Shanahan, M., Carré, A., Spreading and dynamics of liquid drops involving nanometric deformations of soft substrates, *Colloids Surf. A* 206 (2002), 115-123
- Singh, K., Lister, J.R., Vella, D., A fluid-mechanical model of elastocapillary coalescence, *J. Fluid Mech.* 745 (2014), 621-646
- Sokuler, M., Auernhammer, G.K., Roth, M., Liu, C.J., Bonaccurso, E., Butt, H.-J., The softer the better: fast condensation on soft surfaces, *Langmuir* 26 (2010), 1544-1547
- Srikar, R., Gambaryan-Roisman, T., Steffes, C., Stephan, P., Tropea, C., Yarin, A., Nanofiber coating of surfaces for intensification of spray or drop impact cooling, *International Journal of Heat and Mass Transfer* 52 (2009), 5814-5826

- Starov, V.M., Zhdanov, S.A., Kosvintsev, S.R., Sobolev, V.D., Velarde, M.G., Spreading of liquid drops over porous substrates, *Advances in Colloid and Interface Science* 104 (2003), 123-158
- Stephan, P., Busse, C.A., Analysis of the heat transfer coefficient of grooved heat pipe evaporator walls, *Int. J. Heat Mass Transf.* 35 (1992), 383-391
- Style, R.W., Jagota, A., Hui, C.Y., Dufresne, E.R., Elastocapillarity: surface tension and the mechanics of soft solids, *Annu. Rev. Condens. Matter Phys.* 8 (2017), 99-118
- Tanaka, T., Morigami, M., Atoda, N., Mechanism of resist pattern collapse during development process, *Japan. J. Appl. Phys.* 32 (1993), 6059-6064
- Thammanna Gurumurthy, V., Rettenmaier, D., Roisman, I.V., Tropea, C., Garoff, S., Computations of spontaneous rise of a rivulet in a corner of a vertical square capillary, *Colloids Surf. A* 544 (2018a), 118-126
- Thammanna Gurumurthy, V., Roisman, I.V., Tropea, C., Garoff, S., Spontaneous rise in open rectangular channels under gravity, *J. Colloid Interface Sci.* 527 (2018), 151-158
- Trybala, A., Starov, V., Kinetics of spreading and wetting of blood over porous substrates, *Curr. Opin. Colloid Interface Sci.* 36 (2018), 84-89.
- Washburn, E.W., The dynamics of capillary flow, *Phys. Rev.* 17 (1921), 273-283
- Weickgenannt, C.M., Zhang, Y., Sinha-Ray, S., Roisman, I.V., Gambaryan-Roisman, T., Tropea, C., Yarin, A.L., Inverse-Leidenfrost phenomenon on nanofiber mats on hot surfaces, *Phys. Rev. E* 84 (2011b), 036310
- Weijs, J., Andreotti, B., Snoeijer, J., Elasto-capillarity at the nanoscale: on the coupling between elasticity and surface energy in soft solids, *Soft Matter* 9 (2013), 8494–8503
- Wenzel, R.N. 1936, Resistance of solid surfaces to wetting by water, *Ind. Eng. Chem.*, v. 28, pp. 988-994
- White, L., The contact angle on an elastic substrate. 1. The role of disjoining pressure in the surface mechanics, *J. Colloid Interface Sci.* 258 (2003), 82-96.

4 Requested modules/funds

4.1 Funding for stuff

1 doctoral researcher or comparable, 100%	36 months
1 student research assistant , 19h/week	36 months, 1143 €/month

The doctoral researcher will be responsible for performing the research work packages under the supervision of Prof. Tatiana Gambaryan-Roisman. He/she will develop the models and implement them into numerical codes, perform the simulations and validate their results by comparison with experimental data and with the numerical results obtained by alternative methods, perform the parameter studies, analyze the results, report the results in form of publications and present them at conferences and at the SPP events. The PhD students at Mechanical Engineering faculty are normally hired for 100% WMA positions. Due to present economic situation the university must compete with numerous potential employers for the Master degree holders. Offering full WMA positions is the only option allowing to attract the potential doctoral researchers.

The student research assistant will support the doctoral researcher by the performance of the simulation and the analysis of the results.

4.2 Funding for direct project costs

4.2.1 Equipment up to €10000, software and consumables

1. Data storage mediums, interlibrary loans	3000,- €
2. Software licenses for Mathematica/Comsol	4000,- €

Total 4.2.1 7000,- €

4.2.2 Travel

1. 2 SPP workshops, 2 persons	2400,- €
2. SPP Advanced school (1 st year), PhD candidate workshop (2 nd year), 1 person	1300,- €
3. SPP international conference (3 rd year), 2 persons	1500,- €
4. Project meetings in the framework of bilateral cooperation	2000,- €

5. Presentation of project results at national and international conferences 6000,- €

Total 4.2.2 13200,- €

4.2.3 Publication costs

750,- € for the 2nd and 3rd years 1500,- €

Total 4.2.3 1500,- €

Total direct project costs:

21 700,- €

5 Project requirements

5.1 Employment status information

Gambaryan-Roisman, Tatiana, Apl. Professor, permanent employment at TU Darmstadt

5.2 First-time proposal data

Not applicable

5.3 Composition of the project group

- Apl. Prof. Dr. Sc. Tatiana Gambaryan-Roisman - project management and supervision
- Prof. Dr.-Ing. Peter Stephan, chair holder - advice in the questions of thermodynamics
- Dr. Frank Dammel, academic director - advice in numerical methods

5.4 Cooperation with other researchers

5.4.1 Researchers with whom you have agreed to cooperate on this project

See Section 2.8

5.4.2 Researchers with whom you have collaborated scientifically within the past three years

- Dr. rer. nat. Elmar Bonaccurso, Airbus Defense and Space GmbH, München
- Prof. Thodoris Karapantsios, Aristotle University of Thessaloniki
- Prof. Dr.-Ing. habil. Eugeny Kenig, Lehrstuhl für Fluidverfahrenstechnik, Fakultät für Maschinenbau Universität Paderborn
- Prof. Dr.-Ing. Jens-Peter Majschat, Professur Verarbeitungsmaschinen/ Verarbeitungstechnik, Technische Universität Dresden
- Prof. Victor Starov, Department of Chemical Engineering, Loughborough University, Loughborough, UK
- Dr. Joachim Venzmer, Evonik Nutrition & Care GmbH, Essen
- Prof. Dr.-Ing. habil. Stefan aus der Wiesche, Fachbereich Maschinenbau, Fachhochschule Münster, Münster
- Prof. Alexander Yarin, University of Illinois at Chicago, Chicago, USA

5.5 Scientific equipment

For the implementation of the project the Lichtenberg High Performance Computer of TU Darmstadt will be available (hardware with 780 and 632 compute nodes). For the validation experiments, two experimental setups are available, which allow the control of the gas atmosphere and temperature, creation of drops of around 1mm size impacting or gently positioned onto a surface as well as optical observation of the drop form evolution and evolution of imbibed area. Several high speed cameras and telecentric lenses are available.

6 Additional information

The DFG Liaison Officer at TU Darmstadt, Professor Dr.-Ing. Johannes Janicka has been informed about this application.

7 Appendices

Academic curriculum vitae

[CV_PubList_Gambaryan_Roisman.pdf](#)